International Journal of Engineering Trends and Technology
ISSN: 2231 – 5381 /doi:10.14445/22315381/IJETT-V69I2P228
Volume 69 Issue 2, 201-206, February 2021

Adaptive Control Techniques Integrated to Grid-Connected RES with Harmonic Filter Capabilities

Gopala Venu Madhav[#1], C. Nagamani[#2], B. Nageswara Rao[*3]

[#]*Assoc. Professor, Dept. of EEE, Anurag University Venkatapur, Ghatkesar, Medchal Dist., Telangana, India*
[*] *Asst. Professor, Dept. of EEE, Anurag University Venkatapur, Ghatkesar, Medchal Dist., Telangana, India*

[1] venumadhaveee@cvsr.ac.in, [2] nagamanieee@cvsr.ac.in, [3] nageswararaoeee@cvsr.ac.in

***Abstract* —** *In this paper, a RES like PVA or wind farm is interconnected to the grid with positive phase sequence synchronization with three-phase voltages of the grid. The interconnection of the RES through VSI injects active and reactive powers and also mitigates harmonics generated by the non-linear load which is connected to the conventional source. An analysis is carried out with a comparison of different controllers of VSI with PI, FOPI, and SMPI gain controllers detecting the values of peak overshoot in DC voltage, THD, and power factor of the source. The control structure efficiency is analyzed with conditions like change in load or change in RES power generation. All the graphs are plotted using the 'powerful toolbox with respect to time in MATLAB Simulink software.*

Keywords — *RES (Renewable Energy Source), PVA (Photo Voltaic Array), VSI (Voltage Source Inverter), PI (Proportional and Integral), FOPI (Fractional Order Proportional and Integral), SMPI (Sliding Mode Proportional and Integral), GUI (Graphical User Interface), THD (Total Harmonic Distortion).*

I. INTRODUCTION

In recent years with the increase in load demand, global warming is also increasing as the power required to meet the load demand is generated by conventional sources [1] using fossil fuels. These conventional sources include coal, diesel, etc., which generate hazardous gases causing global warming. To reduce this problem, the traditional way of generating power needs to be replaced by renewable energy sources [2]. In today's technology, the most efficient renewable sources we have are PVA and wind farms [2]. However, wind farms are a more complicated and huge capital investment that also needs to be connected in parallel with another three-phase source. Wind farms cannot generate power in standalone mode, so they are replaced with PVA renewable sources, which can generate power individually.

In previous papers [3], the modeling of the grid-connected renewable source system is controlled by using hysteresis current loop controllers and conventional PI controllers. The impact on the source voltages and currents is less, and injected power also has many oscillations and peak value generations. This disrupts the DC voltage of the renewable source and also creates harmonic distortions in the waveforms. Most of the inverter source combinations used are PVA-connected systems [3] with DC-DC booster converters. The controllers use unit vector templates to generated reference waveforms for the comparison in hysteresis current loop controllers.

The produced DC power by PVA RES is inverted to 3-ph AC using the PWM technique and is integrated into the grid in parallel with the LCL filter connected between the inverter and grid [4]. The LCL filter mitigates the harmonics caused by the VSI and compensates the current harmonics of the conventional source. As the solar irradiation (Ir Watts/mt^2) and ambient temperature (T ^{0}C) are not constant throughout a day, the DC voltage of the PVA is also not constant. This disturbed DC voltage produced from PVA cannot be integrated into the grid directly. Hence a DC-DC voltage stabilizing booster converter is connected between PVA and inverter for DC voltage stabilization.

The test system considered to interconnect RES is rated at 415V 50Hz with non-linear loads connected on the receiving end side. The non-linear loads are power converters that consume unbalanced currents by converting AC to DC from the source, generating harmonics injected into the source current and voltage. The RES-connected VSI is integrated at PCC, which eliminates the harmonics caused by the unbalanced non-linear load and also compensates active and reactive power consumed by the load. A PVA 3-ph grid integration schematic diagram is given in Fig. 1.

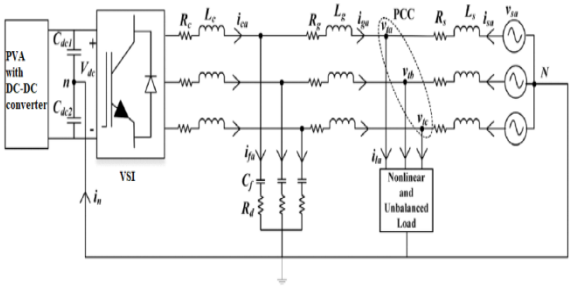

Fig. 1: Grid interconnected PVA RES with unbalanced non-linear load

To control the six IGBT switches of VSI, an SRF (Synchronous Reference Frame) current controller [5] [6] is used with the sinusoidal PWM technique used to generate PWM (Pulse width modulation) pulses for the IGBTs. The internal structure of PVA with DC-DC

converter and internal modeling of VSI [6] can be seen in Fig. 2 below.

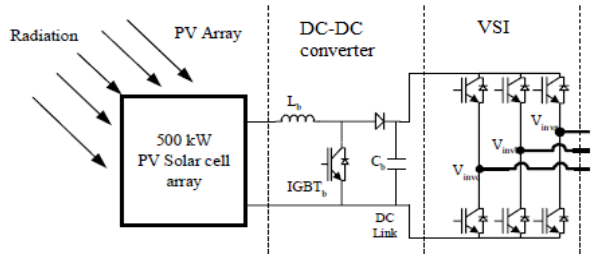

Fig. 2: PVA with DC-DC converter connected to six switch VSI

The DC-DC converter has a single IGBT which is controlled by a voltage-oriented feedback controller [7], which maintains the DC voltage output of the converter at the desired voltage level. The voltage output from the controlled DC-DC converter is fed to VSI, which is controlled by the SRF method control structure [10]. The modeling of the PVA-connected VSI is explained in different sections with control structures used are given in Section II, and in Section III SRF method working principle is explained. Section IV contains all comparison Simulink results obtained by using PI, FOPI, and SMPI controllers.

II. CONTROL STRUCTURE

The conventional SRF control includes parks transformation [8] with PI controller controlling the reference values. The proportional gain and Integral gain values are set either by trial and error method [8] or using optimizing techniques. The SRF controller changes only the direct-axis component generated from the comparison of voltage from the DC-DC converter with a reference value. The SRF controller considered for our test system can be seen in Fig. 3.

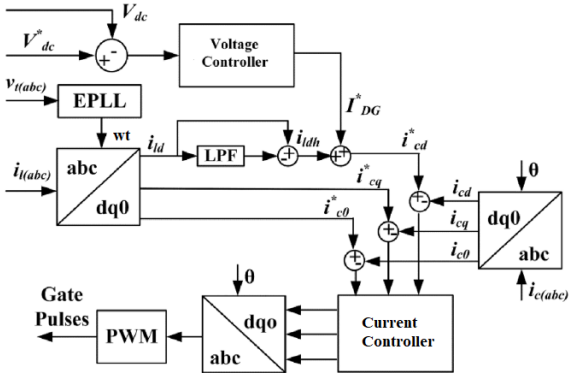

Fig. 3: Proposed SRF controller for RES VSI

In the proposed control to synchronized the VSI with the grid voltage, a PLL [9] (Phase-locked loop) is taken with feedback from source voltage Vg(abc) generating angle (wt) for parks and inverse parks transformations. To get current reference values, Ia* Ib* and Ic* load current IL(abc) is taken, for which parks transformation [10] is applied, generating I_{Ld}, $I_{Lq,}$ and I_{L0}. The d-axis load current component is passed through LPF (low pass filter), eliminating the higher-order harmonics. The low pass filter d-axis component is compared with the d-axis component by feedforward control, and low order harmonics are eliminated, producing a higher-order harmonic d-axis component value, which is given as

$$I_{dh} = I_d - I_{ld} \text{……..(1)}$$

The higher-order d-axis component is added with the DC component parameter generated by a comparison of reference DC voltage and measured DC voltage across the DC-link capacitor from the DC-DC converter. The error is fed to the voltage controller, which can be PI or FOI or SMPI, generating the required d-axis component I^*_{DG} to be added for the I_{dh}. The reference dq0 current components generated from the transformation of the park given as

$$I_{cd}^* = I_{dh} + I^*_{DG} \text{……(2)}$$

$$I_{cq}^* = I_{Lq} \text{ ……..(3)}$$

$$I_{c0}^* = I_{L0} \text{ ……..(4)}$$

These reference currents are compared to dq0 components of VSI current IC (abc) which are generated by applying parks transformation to the VSI currents. The error generated by comparing the reference and measured values of VSI currents is fed to the current controller, which can also be PI or FOPI, or SMPI. The output values V_d^*, V_q^*, and V_0^* from the current controller are transformed to complex abc format using inverse parks transformation generating reference [10] sinusoidal control signals for Sinusoidal PWM generator, producing pulses for the six IGBTs connected in the VSI.

III. CONTROLLERS FOR SRF METHOD CONTROL STRUCTURE

Inactive power filter feedback controllers are mandatory for controlling the power electronic switches of the converter. The pulses are generated using signals produced by the comparison of reference signals and measured signals. The comparison of these signals generates an error that is fed to different controllers. Among these reference value generation modules, the PI controller is considered a traditional controller for the generation of reference control signals.

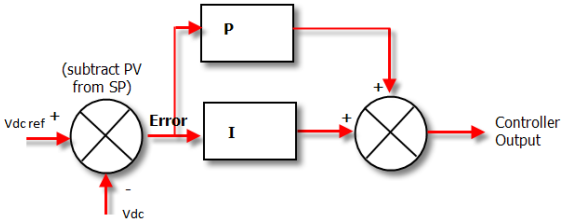

Fig. 4: Conventional PI controller

The PI controller is very sensitive to the error signals generated by the comparison. This sensitive signal generation leads to disturbances and oscillations in the output signals. This issue can be reduced by replacing the regular PI controller with a FOPI [9] (Fraction order proportional-integral) gain controller.

$$G(s) = \frac{Ki\, e^{-Ls}}{\tau s+1} \text{.....(5)}$$

Where τ is processing time constant; Ki is the integral gain of the controller; L is the time delay;

The Kp is kept intact with no change in the value of FOPI. Whereas the integral gain Ki is tuned using the fractional-order derivative transfer function. The disturbance in the value is minimized using a low pass filter for better tuning of the Ki value. The internal modeling of FOPI can be seen in Fig. 5.

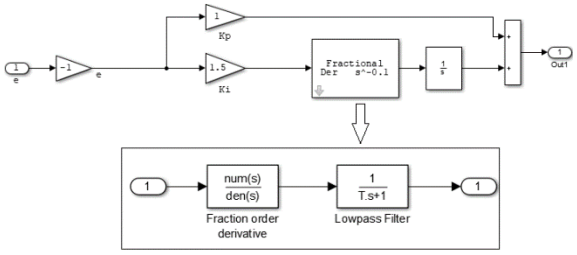

Fig. 5: FOPI internal modeling

With only tuning the Ki value, the disturbances are reduced, but the peak value generation is not eliminated. So, for further advancement of the SRF controller, the FOPI has further been replaced with SMPI [7] (Sliding mode proportional and integral) gain controller. In this controller, the proportional gain (Kp) and integral gain (Ki) is variable with respect to the error input given to the controller. The internal modeling of the SMPI controller can be seen in Fig. 6.

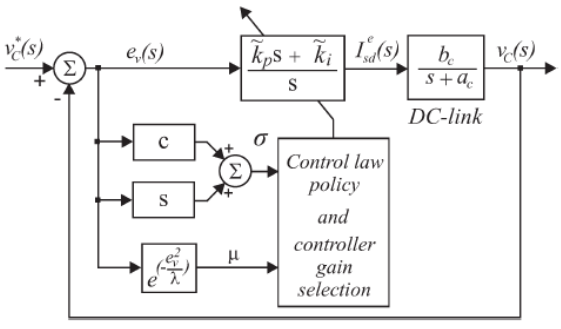

Fig. 6: SMPI controller block diagram

The control law policy varies the Kp and Ki [8] parameters with σ and μ error coefficients. The error coefficient parameters are generated as

$$\sigma = e(s).(c+s) \text{ .....(7)}$$

where e(s) = error from reference DC voltage (Vdc*) and measured DC voltage (Vdc) comparison

c = 10; s = 1;

λ = 300;

The variable Kp and Ki value generation in the sliding mode controller are given as

$$K_p^{\sim} = \left[\left(1+sgn(\sigma)\right)K_p^{+} - \left(1-sgn(\sigma)\right)K_p^{-}\right] + K_p^{avg} \text{ .....(8)}$$

$$K_i^{\sim} = \left[\left(1+sgn(\sigma)\right)K_i^{+} - \left(1-sgn(\sigma)\right)K_i^{-}\right] + K_i^{avg} \text{ .....(9)}$$

The predefined values of positive and negative gains are given in Table I.

TABLE I

K_p^{+}= 0.022	K_p^{-}= 0.011	K_p^{avg}=3
K_i^{+}=1.236	K_i^{-}= 0.72	K_i^{avg}= 0.02

The controller of the DC-DC converter is the PI controller with gains Kp = 0.01 and Ki = 0.0023. This controller and gains are maintained the same for all three SRF controllers. The simulation is carried out for three controllers of the SRF control structure with two cases a) sudden variation in RES output power and b) sudden load variation. Comparative results are shown with respect to dynamic changes in the system. The changes in parameters mentioned in the cases are maintained the same in all three simulations for comparison of graphs plotted.

IV. SIMULINK RESULTS AND OUTPUTS

Case a: Sudden variation in RES output power

The RES output power is varied from 0 to 20kW with an increase in solar irradiation from 0 to 800Watts/mt^{2}at 0.1sec. Grid current improvement along with power injected by the RES sources into the grid can be observed with different environmental conditions.

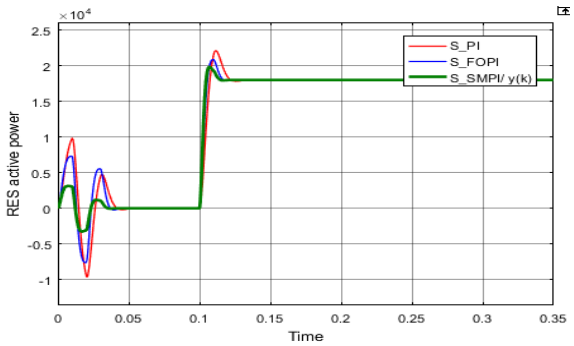

Fig. 7: RES active power comparison for three controllers of SRF

At the initial state, the system is transient, which settles 0.05secs. During this state, the test system works as APF since there is no active power generated on the DC side of the converter. Hence the active power of the source is 10kW which is consumed by the load.

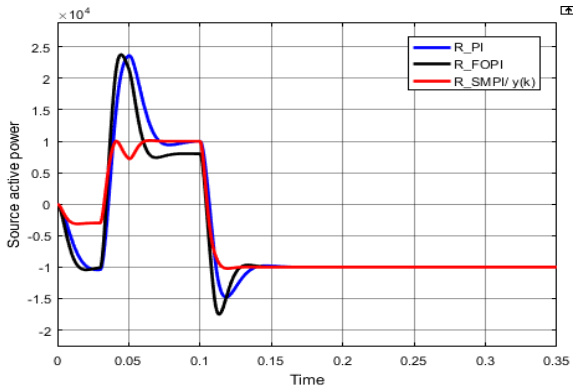

Fig. 8: Source active power comparison for three controllers of SRF

At 0.1sec, when RES is connected at PCC, the load consumes 10kW of power, and the remaining 10kW generated by the RES is injected into the grid, which can be seen in Fig. 10. The transition of source active power from 10kW to -10kW at 0.1sec.

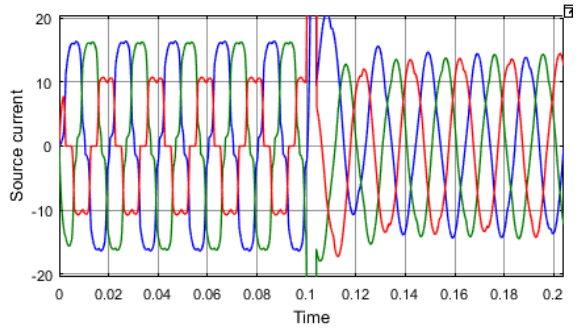

Fig. 9: Source current with the change in RES power at 0.1sec

At 0.1sec, when RES is connected, the source current THD is reduced where the third harmonic content wave is changed to a sinusoidal waveform.

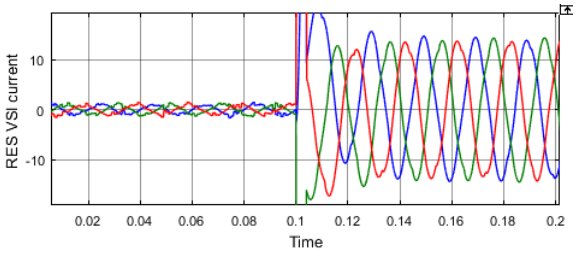

Fig. 10: RES connected VSI current

The above is the current injected by the RES VSI module when there is an increase in solar irradiation at 0.1sec.

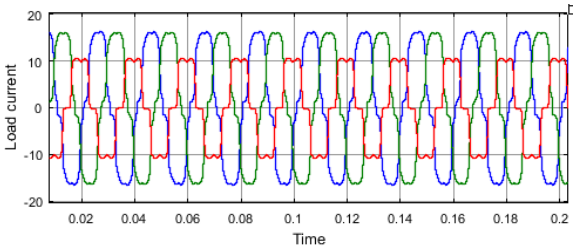

Fig. 11: Load current of unbalanced non-linear load

Irrespective of the change in RES power and source power, the load always consumes constant current either from conventional source or from RES-connected VSI.

Case b: Sudden load change at 0.4sec to 26kW, increase in power generation from RES to 26kW at 0.75sec and decrease in load at 1sec to 18kW.

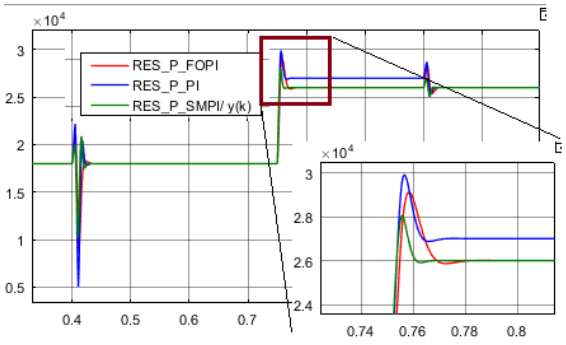

Fig. 12: RES active power comparison of three controllers of SRF

In case 'b,' when the load is changed at 0.4sec from 10kw to 26kW, the extra power of 10kW from RES, which was injected into the grid, is now diverted to load. Even though the RES provides only 20kW, the source also injects the remaining deficit power of 6kW into the load. At 0.75secs, the power from RES is increased with an increase in solar irradiation from 800W/mt^2 to 1100W/mt^2 producing more power which increases from 20kW to 26kW. The load is again decreased to 20kW at 0.75secs, making the extra power of 5kW to be injected into the grid.

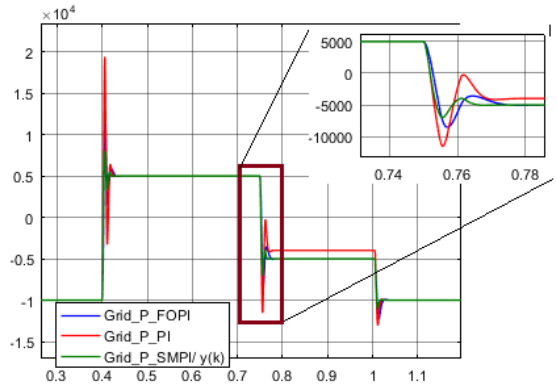

Fig. 13: Conventional source active power comparison of three controllers of SRF

The load is further decreased to 10kW, and irradiation is dropped to 800W/mt^{2,} reducing the power generation of RES to 20kW, where 10kW is consumed by the load and 10kW is injected into the grid.

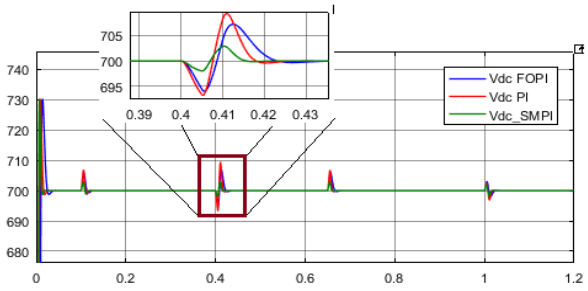

Fig. 14: DC link voltage comparison of VSI with three controllers of SRF

The above figure is the variation in DC link voltage with change in load demand, change in RES power generation with the change in solar irradiation. The voltage is always maintained at 700V with any change in the parameters of the system. A higher voltage variation is observed at 0.4secs because of the large load variation from 10kW to 26kW.

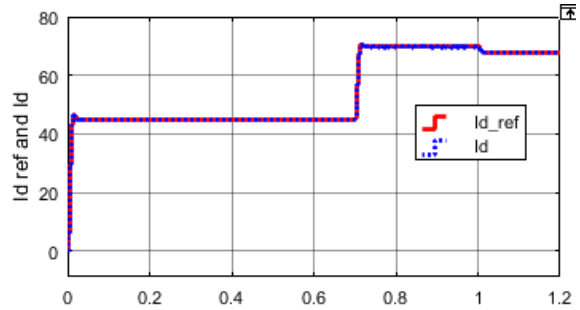

Fig. 15: Id and Idref comparison of SMPI controller for the given power changes

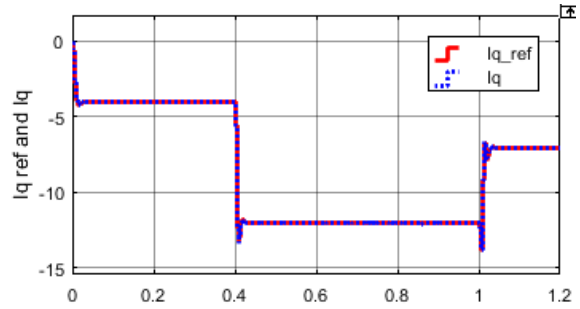

Fig. 16: Iq and Iqref comparison of SMPI controller for the given power changes

The above graphs are d-axis and q-axis component measured and reference value variations of current during a change in load and change in RES power.

A tabular comparison of value is given by analyzing the above graphs generated by a change in parameters, with peak overshoots, power factor during different inductive filter values, and THD (Total Harmonic distortion) of the source currents.

TABLE II

Comparison of the different controller with variable Lc (inductive filter)

Lc (mH)	Setting Time (PI)	Setting Time (FOPI)	Setting Time (SMPI)	% peak Overshoot (PI)	% peak Overshoot (FOPI)	% peak Overshoot (SMPI)	THD (PI)	THD (FOPI)	THD (SMPI)
0.15	**85 ms**	**75 ms**	**60 ms**	**4 %**	**3.3 %**	**2.7 %**	**5.85 %**	**3.3 %**	**2.5 %**
0.24	**92 ms**	**80 ms**	**62 ms**	**3.5 %**	**3%**	**2%**	**3.1 %**	**2.5 %**	**1.8 %**
0.55	**98 ms**	**86 ms**	**65 ms**	**3%**	**2.5 %**	**1.5 %**	**1.8 %**	**1.5 %**	**0.86 %**

In conventional PI controller used RES VSI, the THD values are compared with the change in Kp (Proportional gain) Integral gain (Ki) values and FOPI, SMPI controllers. The values observed are given in TABLE II.

TABLE III

Controller	Power factor	THD %
SMPI	**0.986**	**0.96%**
FOPI	**0.986**	**1.6%**
Kp = 8, Ki = 12	**0.94**	**2.8%**
Kp = 8, Ki = 25	**0.95**	**3.1%**
Kp = 8, Ki = 35	**0.97**	**3.2%**
Kp = 13, Ki = 12	**0.93**	**2.5%**
Kp = 18, Ki = 25	**0.96**	**2.8%**
Kp = 25, Ki = 45	**0.98**	**1.4%**

V. CONCLUSIONS

Analysis of a RES integrated active power filter connected to the grid for reduction of harmonics in source current with different adaptive controllers is shown. The power injected by the RES into the grid with respect to changes in environmental conditions is also observed with respect to time. The power factor of the source and total harmonic distortion of source current are achieved using the FFT analysis tool in MATLAB software. With the tabular comparison can be concluded that the power factor

and harmonic distortion of the source current are minimal in RES connected active power controller by sliding mode PI controller with the continuous tuning of Kp and Ki values with respect to the error generated.

References

[1] Enslin, Johan HR, and Peter JM Heskes., Harmonic interaction between a large number of distributed power inverters and the distribution network. IEEE transactions on power electronics 19(6)(2004) 1586-1593.

[2] Borup, Uffe, Frede Blaabjerg, and Prasad N. Enjeti. "Sharing of nonlinear load in parallel-connected three-phase converters. IEEE Transactions on Industry Applications 37(6)(2001) 1817-1823.

[3] Jintakosonwit, Pichai, Hideaki Fujita, Hirofumi Akagi, and Satoshi Ogasawara. Implementation and performance of cooperative control of shunt active filters for harmonic damping throughout a power distribution system.IEEE Transactions on industry applications 39(2)(2003) 556-564.

[4] Pinto, J. G., Ricardo G. Pregitzer, Luís FC Monteiro, and João L. Afonso. 3-phase 4-wire shunt active power filter with renewable energy interface., (2007).

[5] Blaabjerg, Frede, Remus Teodorescu, Marco Liserre, and Adrian V. Timbus. Overview of control and grid synchronization for distributed power generation systems. IEEE Transactions on industrial electronics 53(5) (2006) 1398-1409.

[6] Carrasco, Juan Manuel, Leopoldo Garcia Franquelo, Jan T. Bialasiewicz, Eduardo Galván, Ramón Carlos PortilloGuisado, MA Martin Prats, José Ignacio León, and Narciso Moreno-Alfonso. Power-electronic systems for the grid integration of renewable energy sources: A survey., IEEE Transactions on industrial electronics 53(4) (2006) 1002-1016.

[7] Rodríguez, Pedro, Josep Pou, Joan Bergas, J. Ignacio Candela, Rolando P. Burgos, and Dushan Boroyevich. Decoupled double synchronous reference frame PLL for power converters control., IEEE Transactions on Power Electronics 22(2)(2007) 584-592.

[8] Soares, Vasco, Pedro Verdelho, and Gil Marques., Active power filter control circuit based on the instantaneous active and reactive current i/sub d/-i/sub q/method., In PESC97. Record 28th Annual IEEE Power Electronics Specialists Conference. Formerly Power Conditioning Specialists Conference 1970-71. Power Processing and Electronic Specialists Conference 1972 2(1997) 1096-1101. IEEE.

[9] Jintakosonwit, Pichai, Hideaki Fujita, Hirofumi Akagi, and Satoshi Ogasawara. Implementation and performance of cooperative control of shunt active filters for harmonic damping throughout a power distribution system., IEEE Transactions on industry applications 39(2)(2003) 556-564.

[10] Pinto, J. P., R. Pregitzer, L. F. C. Monteiro, and J. L. Afonso. 3-phase 4-wire shunt active power filter with renewable energy interface,‖ presented at the Conf., IEEE Renewable Energy & Power Quality, Seville, Spain (2007).

[11] Blaabjerg, Frede, Remus Teodorescu, Marco Liserre, and Adrian V. Timbus., Overview of control and grid synchronization for distributed power generation systems., IEEE Transactions on industrial electronics 53(5)(2006): 1398-1409.